Am J Transl Res 2020;12(8):4371-4383
www.ajtr.org /ISSN:1943-8141/AJTR0103862

Original Article

The etiological role of endoplasmic reticulum stress in acute lung injury-related right ventricular dysfunction in a rat model

Shaolei Ma[1], Yujie Wang[2], Jing Yao[3], Quan Cao[4], Xiangrong Zuo[4]

[1]Department of Emergency and Critical Care Medicine, Zhongda Hospital Affiliated to Southeast University, Nanjing, China; [2]Department of Critical Care Medicine, The Third Affiliated Hospital of Suzhou Medical University, Changzhou, China; Departments of [3]Echocardiography, [4]Critical Care Medicine, The First Affiliated Hospital of Nanjing Medical University, Nanjing, China

Received October 22, 2019; Accepted July 15, 2020; Epub August 15, 2020; Published August 30, 2020

Abstract: This study aimed to ascertain whether endoplasmic reticulum (ER) stress participates in acute lung injury (ALI) and related right ventricular dysfunction (RVD) as well as to explore the underlying mechanisms of these conditions. A single intratracheal instillation of lipopolysaccharide (LPS) (10 mg/kg) was used to establish the RVD model. The ER stress inhibitor, 4-PBA (500 mg/kg), was administered using a gavage 2 hours before and after the LPS treatment for prevention and treatment, respectively. At 12 hours post-LPS exposure, mRNA and protein expressions of ER stress-specific biomarkers, glucose regulating protein 78 (GRP78) and CCAAT/enhancer binding protein homology (CHOP), were significantly upregulated. This effect was inhibited by both 4-PBA prevention and treatment. In addition, echocardiography showed that 4-PBA improved the LPS-induced abnormality in the tricuspid annular plane systolic excursion (TAPSE) and the right ventricular end-diastolic diameter (RVEDD), however not in the pulmonary artery acceleration time (PAAT). Furthermore, hematoxylin and eosin staining (HE) and terminal transferase dUTP nick end labeling (TUNEL) assays revealed that the proportion of proapoptotic cells was higher in RVD rats. This was prominently ameliorated by 4-PBA treatment. Moreover, 4-PBA had a similar reverse effect on the LPS-induced increase in the Bax/Bcl-2 ratio, caspase-12, and caspase-3 expressions as revealed by western blotting. Furthermore, 4-PBA improved LPS-induced right ventricle (RV) myeloperoxidase (MPO)-positive neutrophil infiltration percentage, inhibited nuclear factor kappa B (NF-κB) activity, and reduced the expressions of inflammatory cytokines, TNF-α, IL-1β, and IL-6, in serum and RV. Taken together, our results indicated that ER stress-mediated apoptosis and inflammation might contribute to the development of ALI-related RVD induced by intratracheal LPS instillation. Gavage-administered 4-PBA could improve right ventricle (RV) systolic dysfunction and dilation, plausibly by blocking ER stress.

Keywords: Endoplasmic reticulum stress, 4-phenyl butyric acid, right ventricular dysfunction, acute lung injury, apoptosis, inflammation

Introduction

Acute lung injury (ALI) or acute respiratory distress syndrome (ARDS) are frequently comorbid with hemodynamic instability, which appears to be the leading cause of mortality. One of the significant contributing factors to such hemodynamic instability is concurrent right ventricular dysfunction (RVD) [1]. In the presence of RVD, the decompensated right heart fails to deliver sufficient cardiac output to maintain systemic arterial perfusion and organ oxygen supply, resulting in cardiogenic shock [2]. Prompt diagnosis and treatment of RVD in the presence of ALI/ARDS is of great clinical significance. However, the right ventricle (RV) remains relatively understudied, and the investigation of isolated RVD is difficult owing to its' complex comorbidities.

In a previous study, we successfully established a simplified rat model of RVD via an intratracheal instillation of a single dose of 10 mg/kg lipopolysaccharide (LPS) [3], to explore the pathophysiology of RVD in the context of ALI/ARDS. We also observed RV cardiomyocyte apoptosis

and inflammation injury in this model, both preceding the advent of obvious RV systolic dysfunction and dilation. Apoptosis participates in the pathophysiology of various heart diseases, such as chemotherapy cardiotoxicity, myocardial infarction, ischemic reperfusion injury, and pulmonary arterial hypertension (PAH)-induced right ventricular hypertrophy and fibrosis. The resultant cardiomyocyte damage plays a key role in heart remodeling and dysfunction [4, 5]. RV inflammation has also been demonstrated in impaired RV contractility and maladaptive remodeling [6]. However, the exact contributing role of apoptosis and inflammation in the development of ALI-related RVD has not been elucidated.

Intriguingly, a shared feature of apoptosis and inflammation is endoplasmic reticulum (ER) stress. For example, activation of ER stress-specific caspase-12 leads to an apoptosis cascade independent of mitochondrial damage [7]. ER stress-related unfolded protein response (UPR) affects the activation of the nuclear factor kappa B (NF-κB) signaling pathway at multiple levels [8]. Our previous work illustrated that ER stress could induce cardiomyocyte apoptosis in a rat model with monocrotaline-induced PAH, and the inhibition of ER stress alleviated RV remodeling and dysfunction [9]. Despite the emerging evidence of the detrimental effects of apoptosis and inflammation on the right heart and the fact that an UPR abnormality has been clearly described in various cardiac diseases, including PAH-induced RV remodeling [10], chronic hypoxia-induced cardiac damage [11], and impaired expansion and proliferation during embryonic heart development [12]. ER stress has not yet been considered as a therapeutic target for ALI-related RVD via simultaneous inhibition of both apoptosis and inflammation.

Thus, in this study, we aimed to ascertain whether ER stress participates in ALI-related RVD by regulating apoptosis and inflammation as well as to explore whether the ER stress inhibitor, 4-phenyl butyric acid (4-PBA), has any beneficial effect on the right ventricle.

Materials and methods

Animals and experimental protocol

The study was approved by the Institutional Animal Care and Use Committee of Nanjing Medical University (Approval ID1704019). Male Sprague-Dawley (SD) rats (200 ± 20 g) were obtained from Charles River Laboratories (Beijing, China), and housed at 22-24°C. They were allowed free access to food and water for 7 days prior to the experiment.

The rats were randomized into four groups (n = 15): a control, RVD, 4-PBA prevention, and 4-PBA treatment groups. The ALI-related RVD rat model was established by a single intratracheal instillation of 10 mg/kg LPS (Sigma Aldrich, USA, L2630, from E. coli 0111: B4). The rats in the control group received an equal volume of normal saline. The ER stress-specific inhibitor, 4-PBA (500 mg/kg) (Sigma Aldrich, USA) was administered using a gavage 2 hours before and after LPS instillation in the prevention and treatment groups, respectively.

At 12 hours after the LPS instillation, RV morphology and function were examined using echocardiography following an intraperitoneal injection of ketamine (75 mg/kg). Then, the rats were sacrificed by decapitation and their RV tissue and serum samples were collected. Hematoxylin and eosin staining, terminal transferase dUTP nick end labeling (TUNEL) staining, and myeloperoxidase (MPO) neutrophil staining were performed using the tissue slices. The mRNA expression of the ER stress response proteins, glucose regulated protein 78 (GRP78) and CCAAT/enhancer binding protein homology (CHOP), was measured using quantitative reverse transcriptase polymerase chain reaction (qRT-PCR). Furthermore, the protein expressions of GRP78, CHOP, and the apoptotic proteins, including Bax, Bcl-2, caspase-12, and caspase-3, were examined by western blotting. RV NF-κB activity was detected using an electrophoretic mobility shift assay (EMSA), and the RV and serum levels of TNF-α, IL-1β, and IL-6 were examined using enzyme-linked immunosorbent assay (ELISA).

Establishment of the RVD rat model

The RVD rat model was established as previously described [3]. Briefly, after intraperitoneal injection of pentobarbital sodium (40 mg/kg); (Shanghai Haling Biotechnology Co., Ltd., Shanghai, China), with an improved human otoscope, a blunt stainless-steel needle was used to instill either LPS or saline into the proximal trachea of the rats. After instillation, the rats were mechanically ventilated (Inspira Asv

Ventilator, Harvard Apparatus Inc., Holliston, America, tidal volume 2 mL, frequency 75 strokes/min) for better drug distribution for approximately 1 minute. They recovered in a warm environment with good ventilation and were observed carefully.

Echocardiography

Transthoracic two-dimensional, M-mode, and Doppler echocardiographic imaging were performed using a M10S detector (10-11.5 MHz) on a Vivid Dimension 7 ultrasound diagnostic machine (General Motors Co., USA), the image depth was adjusted to 2-4 cm. The following parameters were detected: pulmonary artery acceleration time (PAAT) [13], tricuspid annular plane systolic excursion (TAPSE) [14], right ventricular end-diastolic diameter (RVEDD) [15], and right ventricular free wall thickness (RVFWT) [16]. These reflected pulmonary hypertension, RV systolic function, RV dilation, and RV hypertrophy, respectively. PAAT was measured from the onset of systolic flow to peak pulmonary outflow velocity and normalized to the cardiac cycle length as measured within the same images. TAPSE of the lateral portion of the tricuspid annular plane was recorded in the M-mode format. RVEDD was measured as the maximal distance from the RV free wall to the septum as observed in the apical four-chamber view. Two-dimensional, short-axis, or long-axis parasternal views, or apical four-chamber views were obtained according to the visualization quality with each parameter averaged from three cardiac cycles.

RV TUNEL staining

RV apoptosis cells were examined using a commercial TUNEL assay kit (In Situ Cell Death Detection Kit, Fluorescein; Roche Diagnostics, Germany) according to the manufacturer's instructions. Briefly, paraffin-embedded sections were dewaxed, digested, and infiltrated. The samples were then incubated in TUNEL solution at 37°C for 2 hours, washed using 4',6-diamino-2-phenylindole (DAPI), and then, stained again. After three washes, the sections were examined using fluorescence microscopy (Zeiss LSM510, Germany) and scanned by CaseViewer 2.2, 3D HISTECH, Ltd. Six micro-fields in each slice and three micro-fields in each rat were analyzed.

RV MPO neutrophil staining

For MPO staining, paraffin-embedded RV sections were sequentially deparaffinized, rehydrated, and antigens were recovered. Endogenous peroxidase activity was blocked by incubation at room temperature (3% v/v) for 25 min in the dark. Then, the sections were sealed with 3% bovine serum albumin for 30 min at room temperature, overnight at 4°C, incubated with primary antibodies (polyclonal goat anti-rat MPO antibody: 1:500, ServiceBio, Wuhan, China), and then, incubated with the corresponding secondary antibodies at room temperature for 50 minutes. Finally, diaminobenzidine was used to observe all sections, and the nuclei were stained using Harris hematoxylin. After dehydration and mounting, the slides were examined using a microscope (Zeiss LSM510, Germany) and scanned using digital microscope application software (CaseViewer 2.2, 3DHISTECH, Ltd). Six microscope fields for each slice and three microscope fields for each rat were analyzed.

Isolation of RNA and qRT-PCR

Total RNA was isolated from the right heart using TRIzol reagent (Invitrogen, CA, USA). Then, cDNA was synthesized using the SYBR real-time PCR master mix kit (Toyobo, Osaka, Japan), according to the manufacturer's instructions. Amplification was performed using an ABI 7000 Taqman system (Applied Biosystems, CA, USA). The relative expressions of GRP78 and CHOP were quantified using the $2^{-\Delta\Delta Ct}$ method. GAPDH expression was analyzed as an internal control. The sequences of the primers used in this study were as follows: GRP78 forward: 5'-ACTGGAATCCCTCCTGCTC-3', reverse: 5'-CAAACTTCTCGGCGTCAT-3'; CHOP forward: 5'-GACAGAGCCAAAATAACAG-3', reverse: 5'-TCACTTTACTGGGTATGGAC-3'; GAPDH forward: 5'-CTCATGACCACAGTCCATGCCA-3', reverse: 5'-GCCTTGGCAGCACCAGTGGATG-3'.

Western blot analysis

Western blotting for GRP78, CHOP, caspase-12, and caspase-3 was performed by incubating the membrane overnight with the corresponding primary antibodies (Cell Signaling Technology, Beverly, MA, USA) at 4°C. After three washes, the membranes were incubated with horseradish peroxidase-conjugated sec-

ondary antibodies for 1 hour. GAPDH (Santa Cruz Biotechnology, CA, USA) was used as a loading control. The relative intensity of bands was then analyzed using enhanced chemiluminescence (ECL, Cell Signaling Technology), visualized using the VersaDoc Imaging System (Bio-Rad, Hercules, CA, USA), and analyzed using NIH Image 1.46 software for band density.

Nuclear protein extraction and electrophoretic mobility shift assay

A commercial kit (Gel Shift Assay System, Promega, Madison, Wisconsin, USA) was used to detect NF-κB activity in RV cardiomyocytes, and the EMSA method was used to detect the DNA binding activity of NF-κB protein in nuclear extracts. In brief, the NF-κB oligonucleotide probe was labeled with [g-32P]-ATP (Free Biotech, Beijing, China) along with T4-polynucleotide kinase. Cardiomyocyte nuclear extracts were incubated with a radio-labeled oligonucleotide probe at room temperature in a gel-binding buffer (Promega) and subsequently resolved using non-denaturing 4% gel electrophoresis in a 0.5% Tris/borate/EDTA buffer. The gels were dried overnight and exposed to the X-ray film (Fuji Hyperfilm). NF-κB activity was quantified by densitometry (Bandleader 3.0 software, Magnitec Ltd., Israel), and the background density was normalized by band density. Unradiolabeled sense and mutated oligonucleotides served as controls.

Enzyme-linked immunosorbent assay

ELISA was used to quantify the expressions of TNF-α, IL-1β, and IL-6 in the RV and serum. Partially frozen RV tissue was homogenized rapidly in a pre-cooled phosphate butter (pH: 7.4) and centrifuged for 10 min at 5,000 rpm at 4°C. The supernatant was collected and the cytokine content was detected using an ELISA kit (Nanjing Jiancheng Co., Ltd.), according to the manufacturer's instructions. The expressions of serum TNF-α, IL-1β, and IL-6 were examined using the same method.

Statistical analysis

Data were expressed as mean ± standard error mean (SEM) and analyzed using one-way analysis of variance followed by Bonferroni post-hoc comparison with GraphPad Prism 8.0 software (Graph Pad Software Inc., San Diego, CA). A $P < 0.05$ was considered to be statistically significant.

Results

Survival status of rats in each group

No deaths were observed in the control group. However, rats in the RVD model group gradually presented respiratory distress, tachypnea, and cyanosis after LPS instillation. Three rats died during the experiment. Finally, only 13 rats survived in the 4-PBA prevention and treatment groups, respectively.

4-PBA prevention or treatment blocked LPS-induced RV cardiomyocyte ER stress

To identify whether ER stress participated in the RVD induction, we detected the mRNA and protein expressions of ER stress-specific molecules, GRP78 and CHOP, using qRT-PCR and western blot, respectively. GRP78 is a Ca^{2+}-dependent molecular chaperone essential for UPR to remove misfolded proteins. However, prolonged or excessive UPR can eventually trigger cell damage. It is one of the markers of ER stress [17]. CHOP is a transcription factor that is activated at multiple levels during ER stress. Under physiological conditions, CHOP is widely expressed at very low levels, and only in the presence of severe or persistent ER stress is its' expression is upregulated. In the present study, mRNA, and protein expressions of GRP78 and CHOP were significantly increased in the RVD model group compared to the control group, indicating that ER stress was activated after LPS instillation. In addition, both 4-PBA prevention and treatment could effectively block the upregulation of these genes. 4-PBA is a low molecular weight fatty acid that stabilizes protein conformation, prevents misfolded protein aggregation, and alleviates ER stress to ameliorate cell damage [18]. All of these findings, as shown in **Figure 1**, suggested that ER stress might play an essential role in the injured RV in RVD rats.

4-PBA improved LPS-induced RV systolic dysfunction and dilation, however not pulmonary hypertension

To further ascertain whether ER stress was involved in the abnormal RV morphology and function after LPS instillation, we assessed

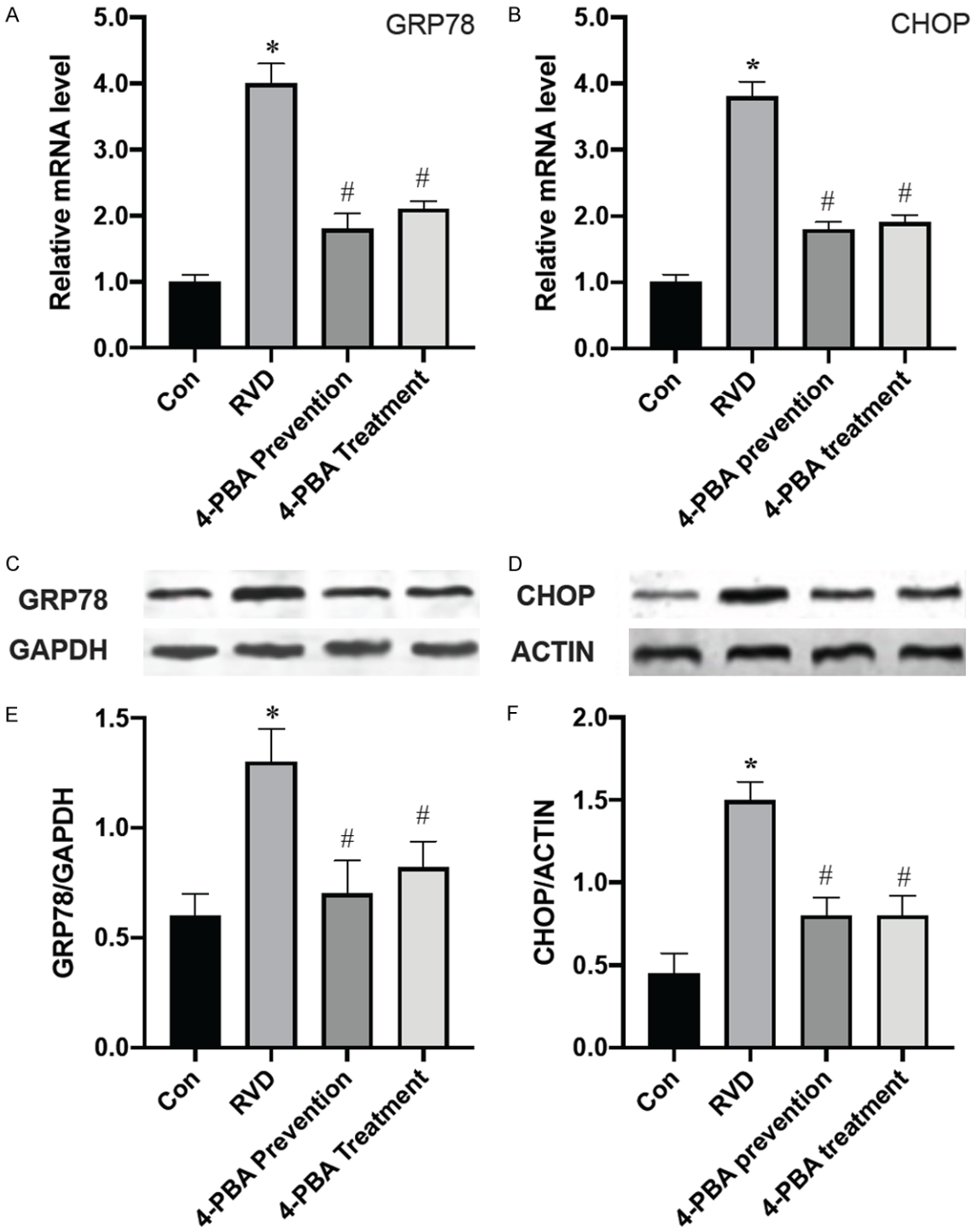

Figure 1. LPS intratracheal instillation induced obvious RV cardiomyocyte ER stress, which could be blocked by either 4-PBA prevention or treatment. An RVD rat model was established with intratracheal instillation of LPS 10 mg/kg. The ER stress inhibitor, 4-PBA (500 mg/kg), was administered using a gavage 2 hours before and after LPS in the prevention and treatment groups, respectively. (A, B) Relative expressions of GRP78 and CHOP mRNAs were detected using qRT-PCR. (C, D) Western blot bands of GRP78 and CHOP, with statistical results shown in (E and F), respectively. Data are presented as mean ± SEM and analyzed by ANOVA followed by Bonferroni post-hoc comparison. $^{*}P < 0.05$ vs. con group; $^{\#}P < 0.05$ vs. RVD group, n = 3 in each group.

echocardiography parameters, PAAT, TAPSE, RVEDD, and RVFWT. PAAT, an indicator of pulmonary hypertension, was shortened in the RVD model rats (23.8 ± 4.87 ms versus 30.01

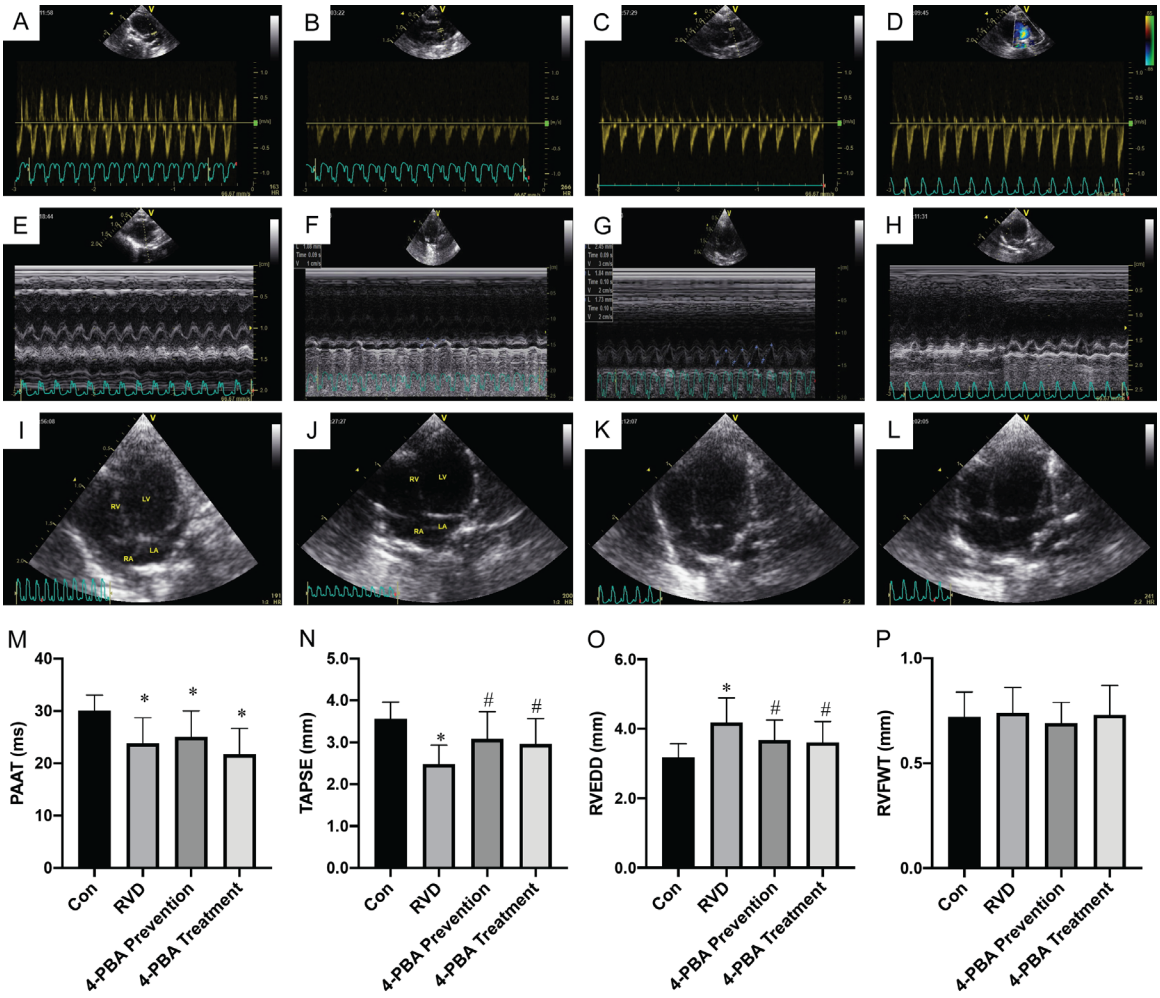

Figure 2. 4-PBA improved LPS-induced RV systolic dysfunction and dilation. In RVD model rats, we observed a decrease in PAAT, which was not affected by 4-PBA. RV systolic dysfunction and dilation were observed as well, as reflected by a decrease in TAPSE and an increase in RVEDD, respectively. Both these effects could be improved by both 4-PBA prevention and treatment. A-D. Echocardiographic images in the parasternal view of mid-systolic pulmonary artery notching and pulse-wave Doppler. E-H. Representative M-mode measurement of TAPSE in the four groups. I-L. Apical 4-chamber views of rats in the four groups. M-P. Statistical analysis of four echocardiographic parameters, including PAAT, TAPSE, RVEDD, and RVFWT. Data are presented as mean ± SEM and analyzed by ANOVA followed by Bonferroni post-hoc comparison. $^{*}P < 0.05$ vs. con group; $^{\#}P < 0.05$ vs. RVD group, n = 3 in each group.

± 3.02 ms), suggesting an increased in afterload in the RV after LPS instillation (**Figure 2A**, **2B**). Notably, the ER stress inhibitor, 4-PBA did not improve PAAT significantly (**Figure 2C**, **2D**). LPS instillation significantly decreased TAPSE (2.48 ± 0.45 mm versus 3.56 ± 0.40 mm); (**Figure 2E**, **2F**) and increased RVEDD (4.18 ± 0.71 mm versus 3.17 ± 0.40 mm); (**Figure 2I**, **2J**), suggesting obvious RV systolic function damage and dilation. In contrast to PAAT, we observed that both 4-PBA prevention and treatment had a protective effect with respect to TAPSE (**Figure 2G**, **2H**) and RVEDD (**Figure 2K**, **2L**). In addition, RV hypertrophy was not observed in the RVD rats, and there was no difference in RVFWT of the 4-PBA prevention or treatment groups (images not shown).

4-PBA inhibits LPS-induced RV myocardial injury in rats

In addition to RV systolic dysfunction and dilation, HE staining revealed that the arrangement of myocardial cells was more disordered in the cardiac muscle tissue of RVD rats. Both 4-PBA prevention and treatment ameliorated such histological changes (**Figure 3**).

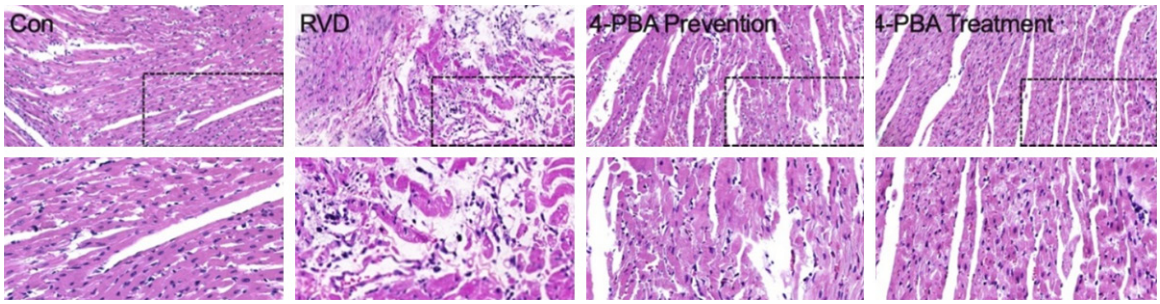

Figure 3. Intratracheal instillation of LPS increased myocardial injury, which could be ameliorated by either 4-PBA prevention or treatment. Representative HE images of the four groups are shown. Scale bar = 50 μm.

4-PBA inhibits LPS-induced TUNEL-positive percentage, Bax/Bcl-2 ratio, and caspase-12 apoptotic pathway activation in rats

Although ER stress is known to be involved in RV systolic function damage and RV dilation, the underlying mechanisms remain unclear. In our previous work, using the same RVD rat model, we observed apoptosis and inflammation in the right heart as early as 6 hours after LPS exposure, preceding the advent of apparent changes in RV morphology and function. Furthermore, one of the ER stress markers, CHOP, is closely related to the increase in the Bax/Bcl-2 ratio [19]. Furthermore, caspase-12 is localized on the cytoplasmic side of the ER membrane, activated under ER stress conditions, followed by caspase-9 and caspase-3 activation [20]. Accordingly, we evaluated the percentage of RV TUNEL-positive cardiomyocytes and the expressions of apoptotic proteins, Bax, Bcl-2, and caspase-12, and caspase-3. As expected, the percentage of RV TUNEL-positive cardiomyocytes (**Figure 4A**) and the expressions of Bax, caspase-12, and caspase-3 increased significantly. However, Bcl-2 expression decreased in the RVD model rats (**Figure 4C-F**). We observed that both 4-PBA prevention and treatment could effectively block such dysregulation in the expressions. This collectively suggested that ER stress might contribute to the apoptosis of the LPS-induced RVD models.

4-PBA improved LPS-induced MPO-positive neutrophil infiltration percentage and inhibited NF-κB activity and expressions of inflammatory cytokines

Inflammation plays a key role in the pathogenesis of cardiomyocyte injury, and its suppression might be an effective intervention strategy. We performed MPO staining to observe neutrophil inflammation infiltration in the four groups. The percentage of MPO-positive neutrophils that infiltrated increased significantly in the RVD rats, while 4-PBA administration ameliorated this effect (**Figure 5A**, **5B**). Inflammation is associated with the expression and regulation of various genes, including NF-κB. In the present study, we observed significant NF-κB signaling pathway activation and upregulation of pro-inflammatory cytokines, TNF-α, IL-1β, and IL-6, in the rats with RVD. Furthermore, 4-PBA inhibited NF-κB activation (**Figure 5C**), partially ameliorated the pro-inflammatory cytokine release of TNF-α, IL-1β, and IL-6 in the RV tissue (**Figure 5D-F**), or totally restored the increased serum cytokine levels (**Figure 5G-I**). These results showed that ER stress was also a critical promoter of inflammation in the rats with RVD. Accordingly, in addition to anti-apoptosis, the anti-inflammatory action of 4-PBA might also be instrumental in its' protective effect against RVD.

Discussion

At present, a contributing factor for mortality and morbidity in patients with ALI/ARDS is concurrent RVD. This highlights the urgent need to explore the underlying mechanisms of this condition and develop therapeutic strategies for RVD. Although physicians have paid great attention to protective strategies, primarily focusing on limiting RV afterload [21], the available treatments continue to be unsatisfactory. Significant cardiomyocyte apoptosis and inflammation were observed in the ALI/ARDS-related RVD rat model, which led to our hypothesis that such pathological changes contribute to damage to RV morphology and function. As expect-

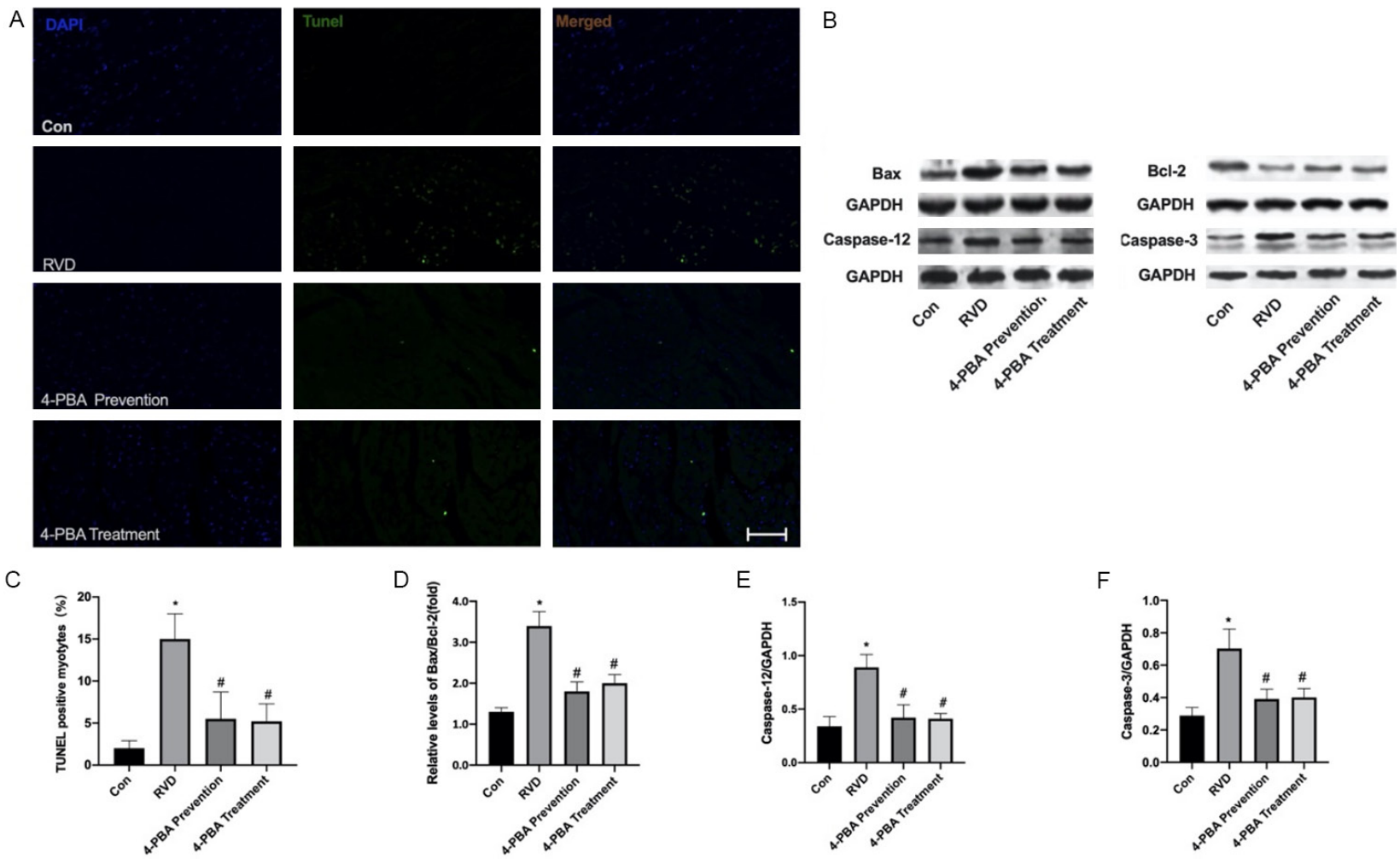

Figure 4. Intratracheal instillation of LPS upregulated TUNEL-positive cardiomyocytes percentage, Bax/Bcl-2 ratio, and expressions of caspase-12 and caspase-3. The effect could be blocked by either 4-PBA prevention or treatment. (A) TUNEL staining of cardiomyocytes in the four groups. (B) Western blots of Bax, Bcl-2, caspase-12, and caspase-3 in the four groups. Statistical analysis of TUNEL-positive myocytes as well as expressions of Bax/Bcl-2, caspase-12, and caspase-3 are shown in (C-F) with data presented as mean ± SEM. $^{*}P < 0.05$ vs. con group; $^{\#}P < 0.05$ vs. RVD group, n = 3 in each group. Scale bar = 50 μm.

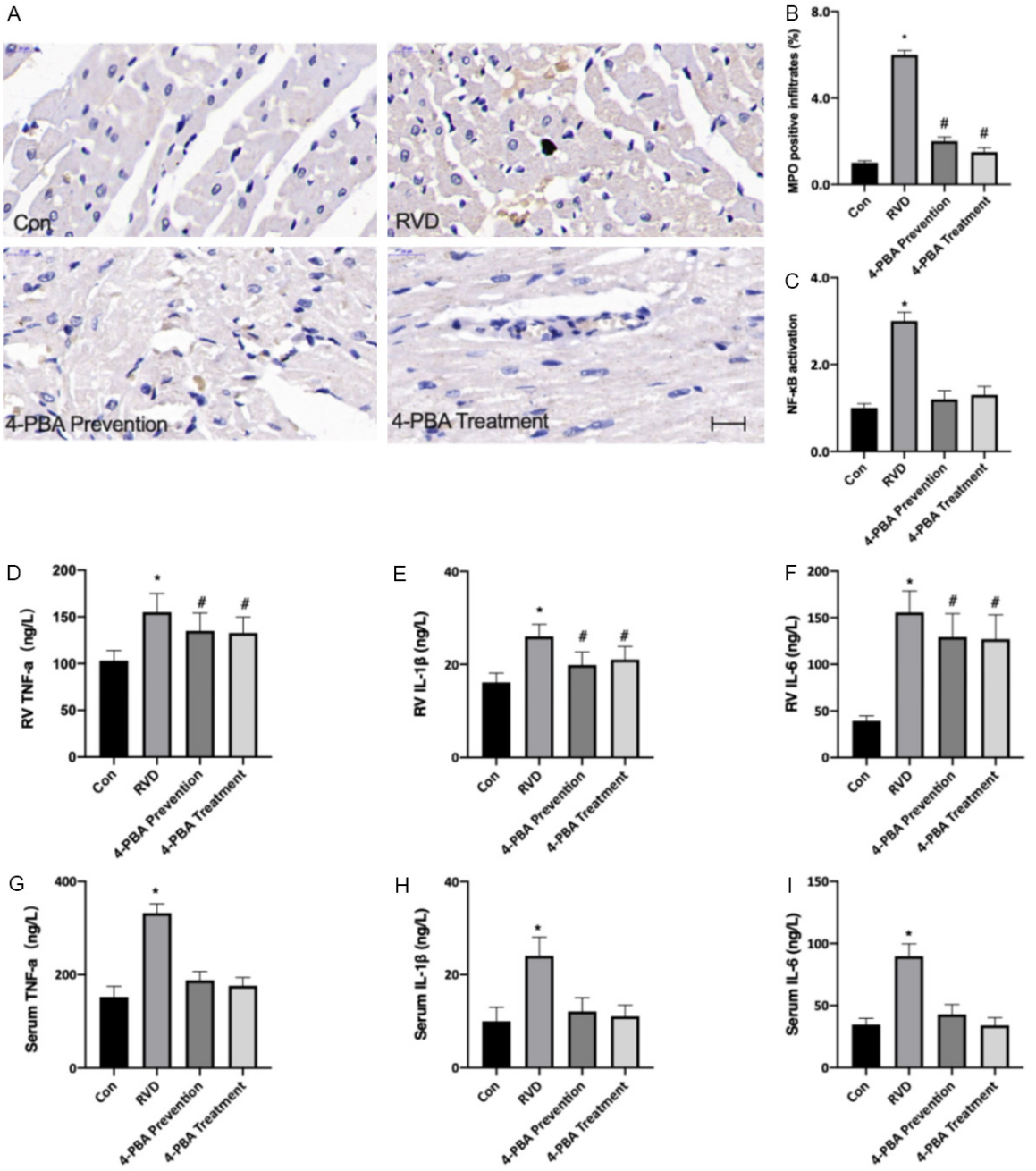

Figure 5. 4-PBA prevention or treatment inhibited LPS-induced MPO neutrophil infiltration, NF-κB signaling pathway activation, and inflammatory cytokine expression. LPS instillation significantly increased RV neutrophil infiltration and upregulated cytokine expression. (A) MPO staining in four groups with statistical analysis shown in (B). (C) RV NF-κB activity. RV and serum cytokine expression are shown in (D-F) and (G-I), respectively. Data in (B-I) are presented as mean ± SEM. $^{*}P < 0.05$ vs. Con group; $^{\#}P < 0.05$ vs. RVD group, n = 3 in each group. Scale bar = 20 μm.

ed, our results showed that ER stress plays a key role in ALI/ARDS-related RVD rats and the ER stress inhibitor, 4-PBA, effectively alleviated apoptosis and inflammation, which led to improvement in the RV systolic function and dilation.

ER stress is known to be an adaptive mechanism by which cells respond to perturbations in ER homeostasis. UPR is mediated by three transmembrane ER signaling proteins, including pancreatic endoplasmic reticulum kinase (PERK), inositol-requiring enzyme I (IRE1), and

activated transcription factor 6 (ATF6) [22]. UPR sensors can trigger changes downstream, signaling factors, such as X-box binding protein 1 (XBP1), CHOP, and eukaryotic translation initiation factor 2 subunit alpha (eIF2a), which further regulate various distinctive UPR target genes to restore ER homeostasis [23]. Unfortunately, if ER homeostasis cannot be restored, a prolonged ER stress response might induce injury.

In human patients and animal models, ER stress is involved in the pathology of various cardiovascular diseases, such as hypertension, ischemic heart diseases, diabetes, and heart failure [24]. ER stress leads to apoptosis and subsequent tissue damage through sensitized mitochondria-dependent apoptotic pathways or the mitochondrial-independent caspase-12 pathway. Although CHOP can increase the Bax/Bcl-2 ratio to promote apoptosis via calcium signaling [25], mitochondrial Bcl-2/Bax can inhibit ER stress-induced apoptosis [26]. Meanwhile, Bax has been reported to localize to the ER to induce apoptosis. Thus, the observed Bax/Bcl-2 ratio after LPS instillation might be the result of a complex interplay between mitochondria and ER. In addition, unlike the Bcl-2 family member, caspase 12 is specific to ER stress-related damage. Its' activation directly cleaves procaspase-9, leading to caspase-9-dependent activation of caspase-3. Both apoptotic pathways were observed in the RV after LPS instillation in our study. Similarly, in the study conducted by Wang et al., in the extended phase of PAH, the ER stress pathway proteins, GRP78, ATF6, IRE1, PERK, and CHOP, were upregulated, along with the emergence of peak apoptosis of RV cardiomyocytes and the ER stress inhibitor, 4-PBA, alleviated remodeling and dysfunction of RV [27]. Clinically, patients with both dilated and ischemic cardiomyopathies show structural and architectural alterations of the ER as well as abnormalities in ER proteins that are involved in the UPR, such as GRP78, XBP-1, and ATF6 [28]. In our study, western blotting showed upregulation in GRP78, CHOP, Bax/Bcl-2 ratio, caspase-12, and caspase-3 in response to intratracheal LPS instillation. Intriguingly, 4-PBA ameliorated these dysregulations and improved RV systolic dysfunction and dilation, strongly indicating that ER stress-mediated apoptosis is an essential mechanism for RVD.

Furthermore, there is a close association between ER stress and inflammation. All three branches of the UPR have the potential to induce NF-κB activation. PERK-mediated translational block is essential for NF-κB activation [29]. IRE1 triggers the NF-κB pathway by binding to TRAF2 [30], and ATF6 might initiate NF-κB-mediated inflammation through AKT phosphorylation [31]. On one hand, activation of the NF-κB signaling pathway results in the transcription of pro-inflammatory cytokines, such as TNF-α, IL-1β, and IL-6, all of which are the most effective mediators of inflammation. Alternatively, ER stress could directly induce an inflammatory response. On the other hand, such inflammatory mediators could further induce ER stress, forming a positive feedback that forms a vicious cycle, amplifying the inflammatory response, and exacerbating cell damage. In our study, we specifically observed increased NF-κB activation and upregulated pro-inflammatory cytokines, TNF-α, IL-1β, and IL-6. All these effects were reversed by 4-PBA, suggesting that ER stress-mediated inflammation might be an alternative mechanism for RVD progression other than apoptosis. We also observed that 4-PBA completely and partially reversed the upregulation in the serum and RV cytokines, respectively. This indicated that some alternative mechanisms that contribute to cardiomyocyte inflammation cannot be completely blocked by 4-PBA. For example, cytokines and LPS also induce overproduction of intracellular reactive oxygen species (ROS), which also function as second messengers, kinases, and transcription factors in a number of signal transduction pathways, such as NF-κB signaling. However, its' role in ALI-related RVD and whether it is susceptible to 4-PBA treatment was not explored in our study and requires further investigation.

We examined echocardiography parameters, TAPSE and RVEDD, to assess RV systolic dysfunction and dilation respectively, both of which were multifactorial, such as pulmonary hypertension or positive pressure ventilation-related afterload increase, or direct contractile function damage on the myocardium [32]. TAPSE is associated with lung injury severity and is an independent predictor of ARDS [33], while RV dilation is a common echocardiographic change in patients with refractory ARDS [34]. Both 4-PBA prevention and treatment partially ame-

liorated, but not totally reversed, abnormal TAPSE and RVEDD, indicating that ER stress might be a contributing factor for RV morphological and functional damage. We also noticed that ER stress inhibitors had no effect on the decreased PAAT after LPS instillation. This indicated that the improvement in RV systolic dysfunction and dilation did not depend on pulmonary hypertension or RV afterload. Similarly, Wang et al. also suggested that although RV dysfunction and failure were highly dependent on the elevated afterload, it also involved complicated, afterload-independent mechanisms [27]. Similarly, during sepsis-induced RV myocardial dysfunction, myocardial inflammation results from LPS-induced sepsis rather than pulmonary hypertension [35]. Taken together, our results strongly suggested that cardiomyocyte apoptosis and inflammation damage *per se,* significantly contributed to the observed RVD in an afterload-independent manner.

Similarly, it is plausible that ER stress triggered the activation of CHOP and the caspase-12 apoptosis pathway as well as NF-κB involved inflammation, the subsequent cardiomyocyte injury, and an abnormality in TAPSE and RVEDD. Targeting the ER stress by activating the adaptive pathway or inhibiting the detrimental pro-apoptotic or pro-inflammatory pathways of the UPR seems to be a beneficial therapy for RVD. 4-PBA was used in our study to provide beneficial treatment effects. In fact, numerous studies have shown a promising therapeutic effect of 4-PBA in individuals with ER stress-related diseases. 4-PBA has a chaperone-like activity and has been shown to attenuate cardiac hypertrophy, fibrosis, and apoptosis in an animal model of pressure overload [36]. Furthermore, in a rat model of heart failure, modulation of ER stress markers, such as GRP78, CHOP, and caspase-12, was proposed to be a mechanism by which atorvastatin protects an individual against heart failure [37]. Importantly, 4-PBA is an FDA-approved chemical chaperone with high translational potential. It may be promising and safer to test 4-PBA in patients with ALI-related RVD.

Taken together, we observed that ER stress led to myocardial apoptosis and inflammation, along with RV morphological and functional changes, all of which could be improved by the ER stress inhibitor, 4-PBA. This emphasized the importance of ER stress inhibition for RV protection. However, based on the available results, there are also unsolved questions in our study. First, whether ER stress signaling is protective or harmful in the right heart continues to be debatable. This shows that a protective or contributing effect must be further elucidated. Second, anti-apoptosis and anti-inflammation are not the only mechanisms for intervention. The complex interplay between ER stress and ROS, miRNAs, or autophagy might shed light on developing alternative therapeutic strategies to rescue ALI-related RVD. Third, the optimal dose of 4-PBA for cardioprotective effects and feasible clinical use remains to be determined.

Acknowledgements

Authors would like to thank the Fundamental Research Funds for the Central Universities (No. 2242019K40255), Priority Academic Program Development of Jiangsu Higher Education Institutions (No. JX10231801), and "Youth Medical Talent" Project in Jiangsu Province (QNRC2016557).

Disclosure of conflict of interest

None.

Address correspondence to: Dr. Xiangrong Zuo, Department of Critical Care Medicine, The First Affiliated Hospital of Nanjing Medical University, Nanjing 21004, China. Tel: +86-25-13913979197; Fax: +86-25-52226112; E-mail: greenboy512@126.com

References

[1] Coz YA, Aguinaga MM, Buch K and Disselkamp M. Hospital and intensive care unit management of decompensated pulmonary hypertension and right ventricular failure. Heart Fail Rev 2016; 21: 323-346.

[2] Biswas A. Right heart failure in acute respiratory distress syndrome: an unappreciated albeit a potential target for intervention in the management of the disease. Indian J Crit Care Med 2015; 19: 606-609.

[3] Ma S, Wang X, Yao J, Cao Q and Zuo XR. Roles of apoptosis and inflammation in a rat model of acute lung injury induced right ventricular dysfunction. Biomed Pharmacother 2018; 108: 1105-1114.

[4] Xia P, Liu Y and Cheng Z. Signaling pathways in cardiac myocyte apoptosis. Biomed Res Int 2016; 2016: 9583268.

[5] Teringova E and Tousek P. Apoptosis in ischemic heart disease. J Transl Med 2017; 15: 87.
[6] Sun X, Abbate A and Bogaard H. Role of cardiac inflammation in right ventricular failure. Cardiovasc Res 2017; 113: 1441-1452.
[7] Morishima N, Nakanishi K, Tsuchiya K, Shibata T and Seiwa E. Translocation of Bim to the endoplasmic reticulum (ER) mediates ER stress signaling for activation of caspase-12 during ER stress-induced apoptosis. J Biol Chem 2004; 279: 50375-50381.
[8] Schmitz ML, Shaban MS, Albert BV, Gokcen A and Kracht M. The crosstalk of endoplasmic reticulum (ER) stress pathways with NF-kappaB: complex mechanisms relevant for cancer, inflammation and infection. Biomedicines 2018; 6: 58.
[9] Wang JJ, Zuo XR, Xu J, Zhou JY, Kong H, Zeng XN, Xie WP and Cao Q. Evaluation and treatment of endoplasmic reticulum (ER) stress in right ventricular dysfunction during monocrotaline-induced rat pulmonary arterial hypertension. Cardiovasc Drugs Ther 2016; 30: 587-598.
[10] Wu Y, Adi D, Long M, Wang J, Liu F, Gai MT, Aierken A, Li MY, Li Q, Wu LQ, Ma YT and Hujiaaihemaiti M. 4-phenylbutyric acid Induces protection against pulmonary arterial hypertension in rats. PLoS One 2016; 11: e0157538.
[11] Jain K, Suryakumar G, Ganju L and Singh SB. Amelioration of ER stress by 4-phenylbutyric acid reduces chronic hypoxia induced cardiac damage and improves hypoxic tolerance through upregulation of HIF-1alpha. Vascul Pharmacol 2016; 83: 36-46.
[12] Rasmussen TL, Ma Y, Park CY, Harriss J, Pierce SA, Dekker JD, Valenzuela N, Srivastava D, Schwartz RJ, Stewart MD and Tucker HO. Smyd1 facilitates heart development by antagonizing oxidative and ER stress responses. PLoS One 2015; 10: e0121765.
[13] Jones J, Mendes L, Rudd M, Russo G, Loscalzo J and Zhang Y. Serial noninvasive assessment of progressive pulmonary hypertension in a rat model. Am J Physiol Heart Circ Physiol 2002; 283: H364-371.
[14] Ghio S, Recusani F, Klersy C, Sebastiani R, Laudisa M, Campana C, Gavazzi A and Tavazzi L. Prognostic usefulness of the tricuspid annular plane systolic excursion in patients with congestive heart failure secondary to idiopathic or ischemic dilated cardiomyopathy. Am J Cardiol 2000; 85: 837-842.
[15] Schenk P, Globits S, Koller J, Brunner C, Artemiou O, Klepetko W and Burghuber O. Accuracy of echocardiographic right ventricular parameters in patients with different end-stage lung diseases prior to lung transplantation. J Heart Lung Transplant 2000; 19: 145-154.
[16] Chemla D, Castelain V, Hervé P, Lecarpentier Y and Brimioulle S. Haemodynamic evaluation of pulmonary hypertension. Eur Respir J 2002; 20: 1314-1331.
[17] Thon M, Hosoi T, Yoshii M and Ozawa K. Leptin induced GRP78 expression through the PI3K-mTOR pathway in neuronal cells. Sci Rep 2014; 4: 7096.
[18] Hwang MS and Baek WK. Glucosamine induces autophagic cell death through the stimulation of ER stress in human glioma cancer cells. Biochem Biophys Res Commun 2010; 399: 111-116.
[19] Matsumoto M, Minami M, Takeda K, Sakao Y and Akira S. Ectopic expression of CHOP (GADD153) induces apoptosis in M1 myeloblastic leukemia cells. FEBS Lett 1996; 395: 143-147.
[20] Galluzzi L, Bravo-San Pedro J and Kroemer G. Organelle-specific initiation of cell death. Nat Cell Biol 2014; 16: 728-736.
[21] Repessé X, Charron C and Vieillard-Baron A. Right ventricular failure in acute lung injury and acute respiratory distress syndrome. Minerva Anestesiol 2012; 78: 941-948.
[22] Hosoi T and Ozawa K. Endoplasmic reticulum stress in disease: mechanisms and therapeutic opportunities. Clin Sci (Lond) 2009; 118: 19-29.
[23] Wang Z, Zhang H, Xu X, Shi H, Yu X, Wang X, Yan Y, Fu X, Hu H, Li X and Xiao J. bFGF inhibits ER stress induced by ischemic oxidative injury via activation of the PI3K/Akt and ERK1/2 pathways. Toxicol Lett 2012; 212: 137-146.
[24] Belmadani S and Matrougui K. Broken heart: a matter of the endoplasmic reticulum stress bad management? World J Cardiol 2019; 11: 159-170.
[25] Diwan A, Matkovich S, Yuan Q, Zhao W, Yatani A, Brown J, Molkentin J, Kranias E and Dorn G. Endoplasmic reticulum-mitochondria crosstalk in NIX-mediated murine cell death. J Clin Invest 2009; 119: 203-212.
[26] McCullough K, Martindale J, Klotz L, Aw T and Holbrook N. Gadd153 sensitizes cells to endoplasmic reticulum stress by down-regulating Bcl2 and perturbing the cellular redox state. Mol Cell Biol 2001; 21: 1249-1259.
[27] Wang J, Zuo X, Xu J, Zhou J, Kong H, Zeng X, Xie W and Cao Q. Evaluation and treatment of endoplasmic reticulum (ER) stress in right ventricular dysfunction during monocrotaline-induced rat pulmonary arterial hypertension. Cardiovasc Drugs Ther 2016; 30: 587-598.
[28] Ortega A, Roselló-Lletí E, Tarazón E, Molina-Navarro M, Martínez-Dolz L, González-Juanatey J, Lago F, Montoro-Mateos J, Salvador A, Rivera M and Portolés M. Endoplasmic reticulum stress induces different molecular structural

alterations in human dilated and ischemic cardiomyopathy. PLoS One 2014; 9: e107635.
[29] Jiang H, Wek S, McGrath B, Scheuner D, Kaufman R, Cavener D and Wek R. Phosphorylation of the alpha subunit of eukaryotic initiation factor 2 is required for activation of NF-kappaB in response to diverse cellular stresses. Mol Cell Biol 2003; 23: 5651-5663.
[30] Hu P, Han Z, Couvillon A, Kaufman R and Exton J. Autocrine tumor necrosis factor alpha links endoplasmic reticulum stress to the membrane death receptor pathway through IRE1alpha-mediated NF-kappaB activation and down-regulation of TRAF2 expression. Mol Cell Biol 2006; 26: 3071-3084.
[31] Zeng L, Liu Y, Sha H, Chen H, Qi L and Smith J. XBP-1 couples endoplasmic reticulum stress to augmented IFN-beta induction via a cis-acting enhancer in macrophages. J Immunol 2010; 185: 2324-2330.
[32] Mitsuo T, Shimazaki S and Matsuda H. Right ventricular dysfunction in septic patients. Crit Care Med 1992; 20: 630-634.
[33] Wadia S, Shah T, Hedstrom G, Kovach J and Tandon R. Early detection of right ventricular dysfunction using transthoracic echocardiography in ARDS: a more objective approach. Echocardiography 2016; 33: 1874-1879.
[34] Lazzeri C, Cianchi G, Bonizzoli M, Batacchi S, Terenzi P, Bernardo P, Valente S, Gensini G and Peris A. Right ventricle dilation as a prognostic factor in refractory acute respiratory distress syndrome requiring veno-venous extracorporeal membrane oxygenation. Minerva Anestesiol 2016; 82: 1043-1049.
[35] Pischke S, Hestenes S, Johansen H, Fure H, Bugge J, Espinoza A, Skulstad H, Edvardsen T, Fosse E, Mollnes T, Halvorsen P and Nielsen E. Sepsis causes right ventricular myocardial inflammation independent of pulmonary hypertension in a porcine sepsis model. PLoS One 2019; 14: e0218624.
[36] Park C, Cha H, Kwon E, Sreenivasaiah P and Kim D. The chemical chaperone 4-phenylbutyric acid attenuates pressure-overload cardiac hypertrophy by alleviating endoplasmic reticulum stress. Biochem Biophys Res Commun 2012; 421: 578-584.
[37] Song X, Yang C, Liu B, Wei Q, Korkor M, Liu J and Yang P. Atorvastatin inhibits myocardial cell apoptosis in a rat model with post-myocardial infarction heart failure by downregulating ER stress response. Int J Med Sci 2011; 8: 564-572.